

CONTROL OF THE MECHANICAL PROPERTIES AND MICROSTRUCTURE OF LASER WELDED JOINTS OF THE ALUMINUM ALLOY V-1461 AFTER HEAT TREATMENT

A.G. Malikov^{1*}, A.M. Orishich¹, E.V. Karpov^{1,2}, I.E. Vitoshkin¹

¹Khristianovich Institute of Theoretical and Applied Mechanics, Siberian Branch, Russian Academy of Sciences,
Institutskaya, 4/1, Novosibirsk, 630090 Russia

²Lavrent'ev Institute of Hydrodynamics, Siberian Branch, Russian Academy of Sciences, Lavrentyeva, 15,
Novosibirsk, Russia 630090

*e-mail: smalik@ngs.ru

Abstract. The paper presents the investigations of the influence of the thermal post-processing on the mechanical characteristics and microstructure of the welded aluminum alloy V-1461 of the system Al-Cu-Li. The temperature and time characteristics of the quenching and artificial ageing processes of the laser welded connections have been optimized in order to have the ultimate tensile stress, yield stress, and relative elongation, as well as the microstructures close to the respective characteristics of the basic alloy. At the optimal modes of the thermal processing, the tensile stress, yield stress and relative elongation of welded samples are 0.92; 0.91 and 0.88, respectively, in respect to the basic alloy values.

Keywords: laser welding, Al-Cu-Li alloy; strength; heat treatment, microstructure

1. Introduction

Aluminum-lithium alloys have low density, the increased elasticity module and high strength as compared to the ordinary aluminum alloys. Today, there are new thermally strengthened wrought aluminum-lithium alloys of the 3rd generation (the system Al-Cu-Li-X (X =Mg, Zn, Mn, Zr, Sc)). These alloys demonstrate high mechanical characteristics (strength, corrosion resistance, impact viscosity), and are the promising materials to be introduced in the aerospace industry [1-3].

Having in mind the purpose to replace riveting widely used in aerospace equipment and hence to reduce the weight of resulting structures, specialists develop intensively different technologies of welding of aluminum-lithium alloys: friction stir welding, laser welding, hybrid laser welding. Laser welding has a number of advantages over the other methods of welding. High speed of the laser welding process, small thermal action zone, as well as the possibility to automate the process make this method the most promising. However the works on the welded joints of the system Al-Cu-Li show that the strength of the welded connections is low and reaches 0.55 – 0.8 of the basic alloy strength [4-6]. Production of high-strength welded connections for the aluminum alloys of the system Al-Cu-Li is an urgent task. To produce the high-strength welded connections, either a wire is used, or the welding process is optimized; the mechanical characteristics, microstructure and phase composition of the welded joint should be studied [7-11].

High mechanical properties of the alloy V-1461 (the system Al-Cu-Li-Mg-X) can be reached after the respective thermal processing (TP), which promotes releasing the strengthening phases T_1 (Al_2CuLi), δ' (Al_3Li), θ' (Al_2Cu), S' (Al_2CuMg) from the solid solution. The presence of rare-earth elements (Sc, Zr) and Ag in the alloy results in the formation of other phases, in particular β' -phase (Al_3Zr), W-phase (on the base of Al, Cu, and Sc), Ω' -phase (on the base of Mg and Ag), $Al_3(Sc, Zr)$, Al_3Sc . These phases form at certain temperatures of the thermal processing and impose their effect on the mechanical properties of the aluminum alloy. The welding process results in the essential changes in these phases composition, solid solution structure and hence changes the mechanical characteristics. Previously in our works [12-15] we showed the effect of the thermal post processing on the laser-welded joint strength for the aluminum-lithium alloys. It is important that the whole sample must be thermally processes. Thus, the modes of the thermal processing influence not only the parameters of the welded joint, but also the initial alloy.

In continuation of our research [12-15], in this study the detailed analysis is done to study the effects of the thermal post-processing modes based on quenching and artificial ageing on the mechanical characteristics (strength) and microstructure of the laser-welded joint of the alloy V-1461 (the system Al-Cu-Li).

2. Materials and Methods

The industrial high-strength aluminum-lithium alloy B-1461, thickness 2 mm, made by Kamensko-Uralskij metallurgical plant (OAO "KUMZ") is based on the system Al-Cu-Li [16-18]. Laser welding was carried out in the ALTC "Sibir 1" including the technological CO_2 -laser, two-coordinate technological bridge-type table which moves the welding torch over the welded sheet. The welding torch includes a focusing ZnSe lens, the gas-dynamic nozzle protecting the welding joint from oxidation, and the mechanism permitting moving the lens position along the beam axis.

The laser radiation was focused on the alloy surface with the ZnSe-lens with the focal distance of 254 mm. The ingots of the aluminum alloys were set on a multi-purpose table with special clamps. The butt welding was carried out. To protect the welded joint and joint root, an inert gas (helium) was supplied through special nozzles. The welding modes optimal for this kind of alloy were: the laser radiation power 3.3 kW, the rate of laser beam motion 4 m/min, focus deepening about the upper sample surface was 3 mm. After the welding, the "dump-bell" samples were made from the ingots for the strength tests in accordance with GOST R ISO 4136-2009. The welded connection strength was measured at the static stretching on the electromechanical tester Zwick/Roell Z100. During the tests, loading and deformation diagrams were recorded by the base of the contact extensimeter (its probes were set into the chamber). For every sample we used the common measurement base of 12 mm approaching to the length of the sample working part.

The samples were thermally processed in the chamber furnace Carbolite equipped with the temperature controller. The samples were quenched at the temperature varying within the range of 320 – 560°C, the heating rate 5°C/min within 30 min, then cooled in cold water and artificially aged at the temperature of 120 – 200°C within 12 – 40 hours. In every case, the whole sample was thermally processes. The microstructures of the welded joint and alloy were tested in the electronic microscope MERLIN Compact Microscope (Carl Zeiss, Germany).

3. Results and discussion

Table 1 presents the major mechanical characteristics of the initial alloy B-1461 of the system Al-Cu-Li in the supply condition and the sample with the welded joint, where σ_{UTS} is the stretching tensile stress, σ_{YS} is the yield stress, δ is the ultimate relative elongation, k_i is the

coefficient showing the ratio of the studied values of the welded joint to the respective values of the initial alloy.

Table 1. Mechanical properties of the welded joint η initial alloy V-1461

Description	σ_{UTS} , MPa	k_1 , %	σ_{YS} , MPa	k_2 , %	δ , %	k_3 , %
Alloy	550	-	470	-	10.1	-
Welded joint	341	62	333	71	0.7	7

It is evident from the data in Table 1 that the welded joint strength decreases dramatically as compared to the initial alloy strength. The TP fulfils the double function. On the one hand, it should increase the mechanical characteristics of the welded joint, but on the other hand, it may influence the basic alloy strength. The full TP complex should guarantee the alloy strength recovery up to the supply condition level. The measurements show that after the quenching up to 320°C, the basic alloy strength reduced from $\sigma_{UTS} = 550$ MPa to $\sigma_{UTS} = 350$ MPa. Figure 1 presents the dependencies of the varying average values of the tensile stress σ_{UTS} , yield stress σ_{YS} , ultimate relative elongation δ for the welded sample on the quenching temperature.

Figure 2 demonstrates these characteristics in relative units; they show the ratio of the resulting values to the respective values of the initial alloy in the supply condition. Here, k_1 is the tensile stress ratio, k_2 is the yield stress ratio, k_3 is the relative elongation ratio to the initial alloy characteristics, respectively. It should be noted that, since the deformation is essentially nonuniform over the length in the welded sample, it is impossible to perform the accurate measurement of the relative elongation with a tensometer. To compare the sample deformation, we used the relative elongation of the working part determined by the movable traverse motion. This value is given below in the graphs as the deformation.

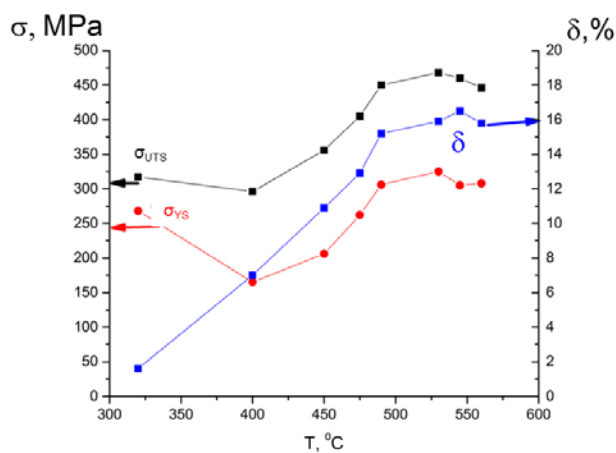


Fig. 1. Dependence of σ_{UTS} , σ_{YS} , δ on the quenching temperature of welded sample

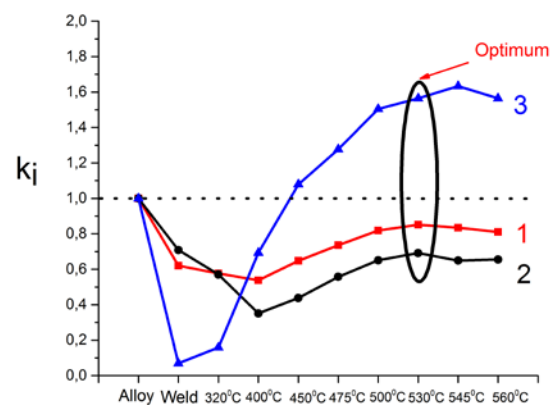


Fig. 2. Dependence of ratios σ_{UTS} (1) $\sigma_{0.2}$ (2) δ (3) of the alloy and welded joint without TP, welded joint with TP as the quenching at different temperatures

Quenching of welded samples causes results in the rise of the tensile stress and elasticity from 341 to 450 MPa (≈ 1.31 times) and from 333 to 400 MPa (≈ 1.20 times). The character of variation of the relative welded joint and welded sample elongation after the quenching at low temperatures of 320 – 450°C depends on the deformation localization predominantly in the joint area; the joint width is on average 1 mm, the other 11 mm cover the basic material inside the base, i.e. the relative elongation in the joint area can in this case

be ~10 times bigger. The given data enable to conclude that the mechanical properties of the joint and surrounding basic material are equal only at high temperatures above 450°C.

As is evident from Fig. 2, the curves of the coefficients k_1 and k_2 have the same behavior character regarding the quenching temperature. At the quenching temperature $T = 530^\circ\text{C}$ they reach their maximums: $k_1 = 0.85$ and $k_2 = 0.69$. To study the effect of different temperature and time characteristics of the artificial ageing process on the mechanical parameters of the samples, two quenching temperatures were chosen: the temperature 530°C, at which the maximal strength characteristics were reached, and the quenching temperature 450°C, at which the characteristic changes appear in the behavior of the curves k_1 , k_2 and k_3 .

Analysis of the effect of the artificial ageing on the mechanical characteristics shows the presence of the optimal quenching temperature. At low quenching temperatures below 500°C, variation of the artificial ageing modes did not lead to any progress in the mechanical characteristics. Figure 3 gives as an example the stress σ versus deformation δ during the stretching of the welded sample quenched at 450°C. It is evident that the sample strength does not change as the ageing temperature varied within the range of 130 – 160°C. The positive role of the artificial ageing process appears at the high quenching temperatures and its optimum was at 530°C. Below we give the variation of the mechanical characteristics at the quenching temperature 530°C and at various artificial ageing modes.

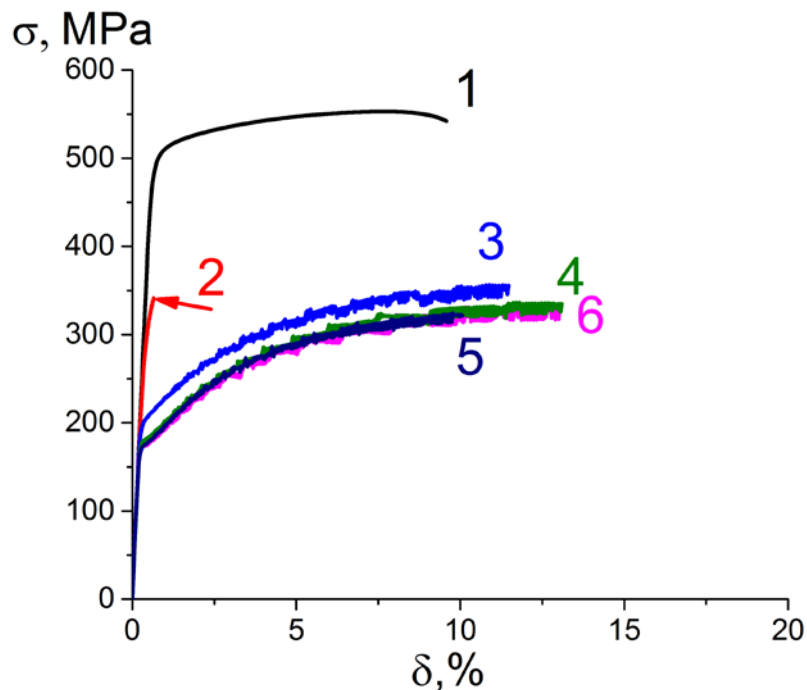


Fig. 3. Stress σ versus deformation δ during stretching
 1 – alloy; 2 – welded joint; 3 – welded joint+quenching at 450°C;
 4 – welded joint + quenching 450°C + ageing at 130°C for 20 hours;
 5 – welded joint + quenching at 450°C + ageing at 150°C for 18 hours;
 6-welded joint quenching 450°C +старение 160°C 16 hours

Figure 4 presents the generalized mechanical characteristics of the samples with the welded joint for the alloy V-1461 of the system Al-Cu-Li versus artificial ageing temperature and time.

3D-maps have been plotted; they result from the approximation of the average values of σ_B (a) $\sigma_{0.2}$ (b) δ (c) on the temperature and time characteristics of the artificial ageing after the quenching at $T=530^\circ\text{C}$; the approximation is carried out by the least-square method. For convenience, the coordinate z of the tensile stress, yield stress, ultimate relative elongation is shown on the right as a color scale. The maps show the maximum areas which are referred as the topographic spine (maximum values area), and the minimum ones referred as the topographic low (minimal values area).

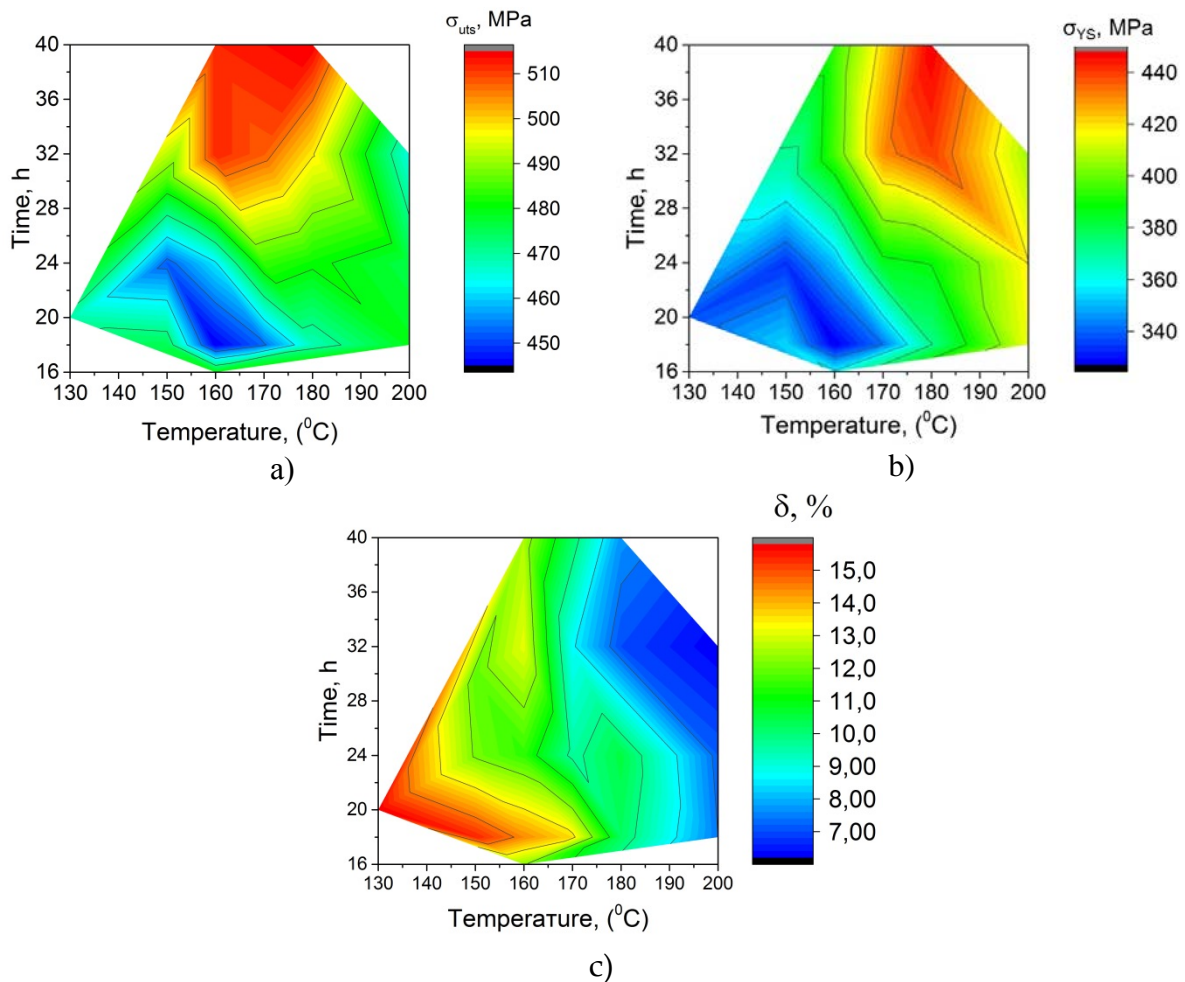


Fig. 4. Mechanical 3D-maps σ_B (a), $\sigma_{0.2}$ (b), δ (c) of the samples with a welded joint

Analyzing Fig. 4, one can see that within the temperature range of $160 - 180^\circ\text{C}$ and time interval of $30 - 40$ hours, there is an evident maximum of σ_{UTS} shaped as a plateau, whereas the maximal values of the tensile stress are $\sigma_{\text{UTS}} = 500 - 510$ MPa, i.e. $91 - 92\%$ of the respective values of the initial alloy in the supply conditions. There is also the evident minimum of σ_B at the artificial ageing temperature of $150 - 170^\circ\text{C}$ and ageing time of $18 - 20$ hours ($450 - 460$ MPa). Similar dependence has been found for the 3D-surface of the welded sample elastic yield. The clear maximum of σ_{YS} is observed at $T = 170 - 190^\circ\text{C}$, the artificial ageing time $32 - 40$ hours, whereas the maximal values of the tensile stress are $420 - 440$ MPa, i.e. $89 - 92\%$ of the respective values of the initial alloy in the supply conditions. The minimum of the elasticity yield is reached at $T = 150 - 170^\circ\text{C}$ and ageing time $16 - 20$ hours, the maximal values of the tensile stress are $330 - 350$ MPa.

On the 3D-surface, the ultimate relative elongation of the welded samples, the minimum of δ (c) is reached at $T = 180 - 200^\circ\text{C}$ within $28 - 34$ hours, the maximal values of the tensile stress δ are (c) = $7.5 - 8\%$, i.e. $74 - 79\%$ of the respective values of the initial alloy in the

supply conditions. The relative elongation maximum is reached at $T = 130 - 140^{\circ}\text{C}$ within 18 – 22 hours, the values δ are (c) = 14 – 15 %, which exceeds the respective values of the initial alloy in the supply conditions by approximately 1.38 times.

The areas of maximal tensile stress and yield stress regarding the temperature and time characteristics of the artificial ageing lie approximately in the same temperature and time range. In the tensile and yield stress maximum area, we observe the zone of ultimate relative elongation decrease (the minimum), and vice versa, in the tensile and yield stress minimum, the relative elongation is maximal. Thus, the data presented in Fig. 4 are pioneering and show the area of control of the mechanical characteristics of the samples from the alloy V-1461 with the laser-welded permanent connection, which results from the thermal processing.

Figure 5 presents the kinetic curves of the regularities in the varying mechanical characteristics of the welded joint at the optimal parameters of the thermal processing (the maximal strength), namely the quenching at $T = 530^{\circ}\text{C}$ within 30 min and the artificial ageing at $T = 170^{\circ}\text{C}$ within 18, 24, 32, and 40 hours; the same Figure shows the values for the alloy in the supply condition and the for the welded joint without thermal processing.

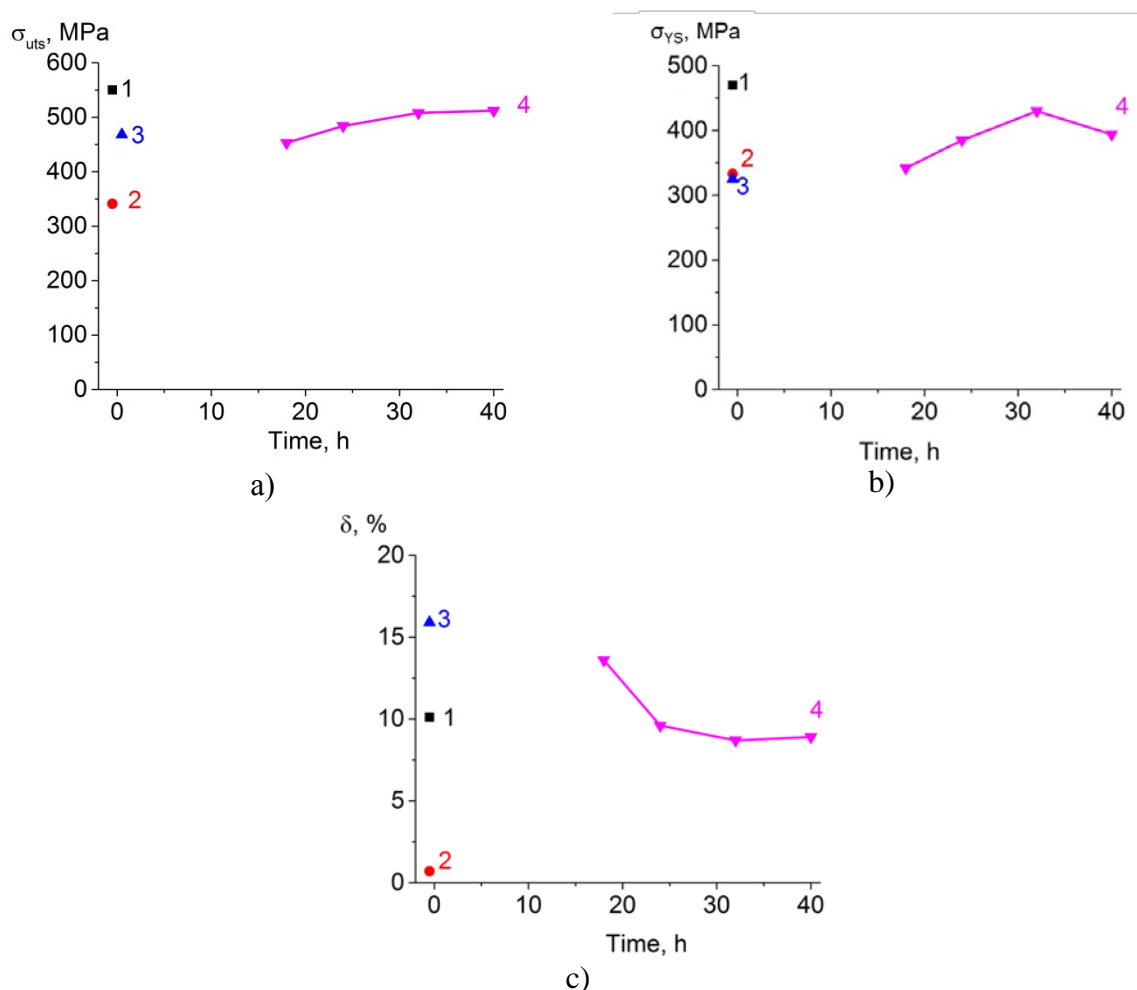


Fig. 5. Kinetic curves of varying σ_B (a), $\sigma_{0.2}$ (b), δ (c) of the welded samples versus the temperature and time characteristics of the thermal processing. 1 – alloy, 2 – welded joint, 3 – welded joint with quenching at 530°C for 30 min, 4 – welded joint with quenching at 530°C for 30 min and artificial ageing, $T=170^{\circ}\text{C}$, 32 hours

Analysis of the data obtained (see Fig. 1 and 5) leads us to the conclusion about the processes making the major contribution in the variation of the mechanical characteristics. Evident that the quenching of the welded samples from the alloy V-1461 at optimal modes results in the essential rise of the tensile stress value from 341 to 468 MPa and does not give any rise of the yield stress. On the contract, the artificial ageing process at the optimal modes increases insignificantly (from 468 MPa to 510 – 512 MPa) the tensile stress and drastically increases the yield stress – from 333 to 440 MPa. The relative elongation of the welded joint jumps from 15.9 % as a result of the quenching process and drops to 8.8 – 9 % after the artificial ageing at the optimal modes.

The physical mechanism of the mechanical characteristics control under the effect of the thermal processing shows the variations in the microstructure. Figures 6 and 7 present the photos of the cross-section slices of the welded samples made by a scanning electronic microscope in the back-scattered electron mode on the micro-level (Fig. 6) and nano-level (Fig. 7), without thermal processing and after the thermal processing at the optimal modes of the quenching ($T = 530^{\circ}\text{C}$, 30 min) and artificial ageing ($T = 170^{\circ}\text{C}$, 32 hours).

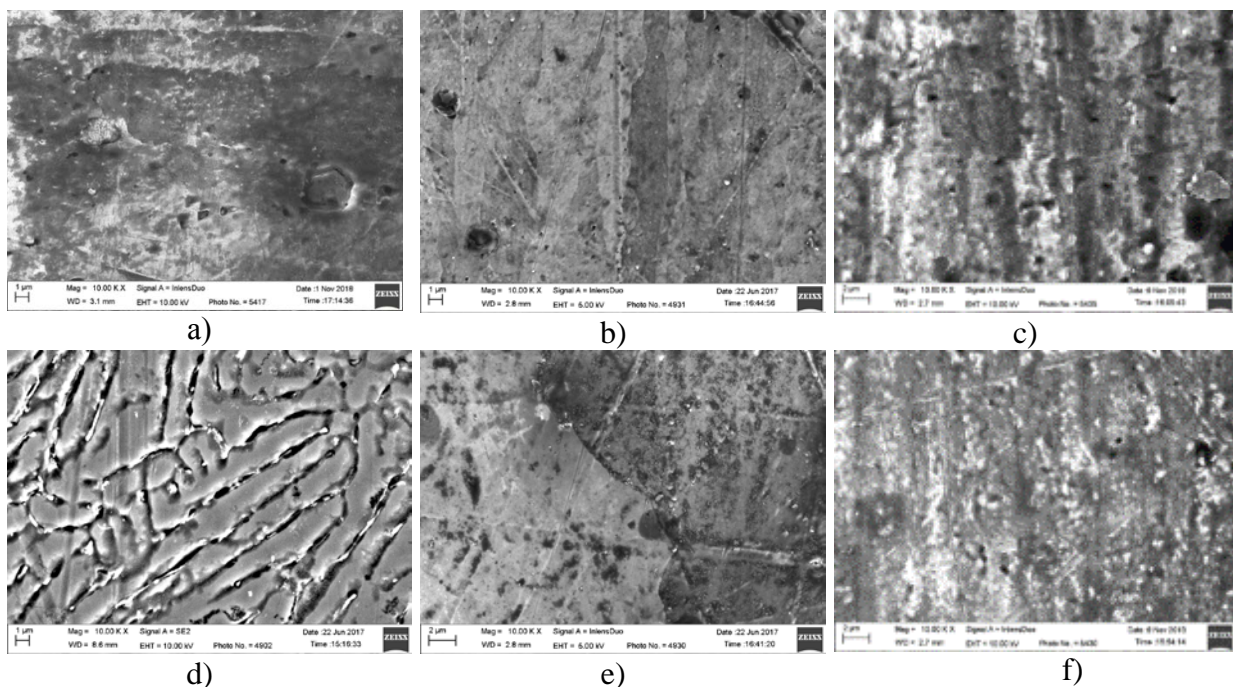


Fig. 6. SEM image of the cross section of the alloy (a, b, c) and welded joint (d, e, f) without thermal processing (a, d), and with it: quenching (b, e), artificial ageing (c, f). Magnification $10\,000^{\times}$

The slice images are made after etching. Nonuniform etching of the slice surface indicates the nonuniform distribution of the basic alloying elements in dendritic cells. In the solid solution of the alloy, light particles with characteristic sizes of 20 – 60 are distributed uniformly (Fig. 6 a). The laser welding makes the structure of the welded joint change (Fig. 6, d and Fig. 7, d). The particles of different phases locate predominantly over the boundaries of the dendritic grains. Due to the evident differences in the morphology and color after etching, two types of insertions can be distinguished: light and dark ones, and often they are combined in complex agglomerates. At the blow-up of $100\,000^{\times}$ one can see that the agglomerates have a complex structure. Inside them the light particles of 20 – 50 nm are seen. The EDX-analysis of the welded joint shows that the content of alloying copper rises up to 11.68 weight % as the copper concentration in the ambient solid solution decreases to 1.2 – 2.2 weight %. Similar data on the copper and other alloying elements (Mg, Li, Zn)

emission are given in [9,10,19,20]. As the quenching temperature rises, the EDX-analysis shows the decrease of the Cu concentration in the dendritic boundary and its increase in the solid solution matrix. To reach the maximal strength of the thermally strengthened alloy B-1461 by means of the controlled heating during the optimal quenching owing to the admixed phase dilution we managed to obtain an intermediate structure which corresponds to the initial stages of the disintegration of the oversaturated solid solution. Thus, the quenching resulted in the non-equilibrium state – the oversaturated solid solution of the alloying elements Cu, Mg and Li in aluminum. The mechanical characteristics were successfully equalized in the alloy and welded joint, and we managed to have at the optimal quenching temperature $T = 530^{\circ}\text{C}$ the maximally homogenized composition of the whole sample (see Fig. 6 and 7, b, e).

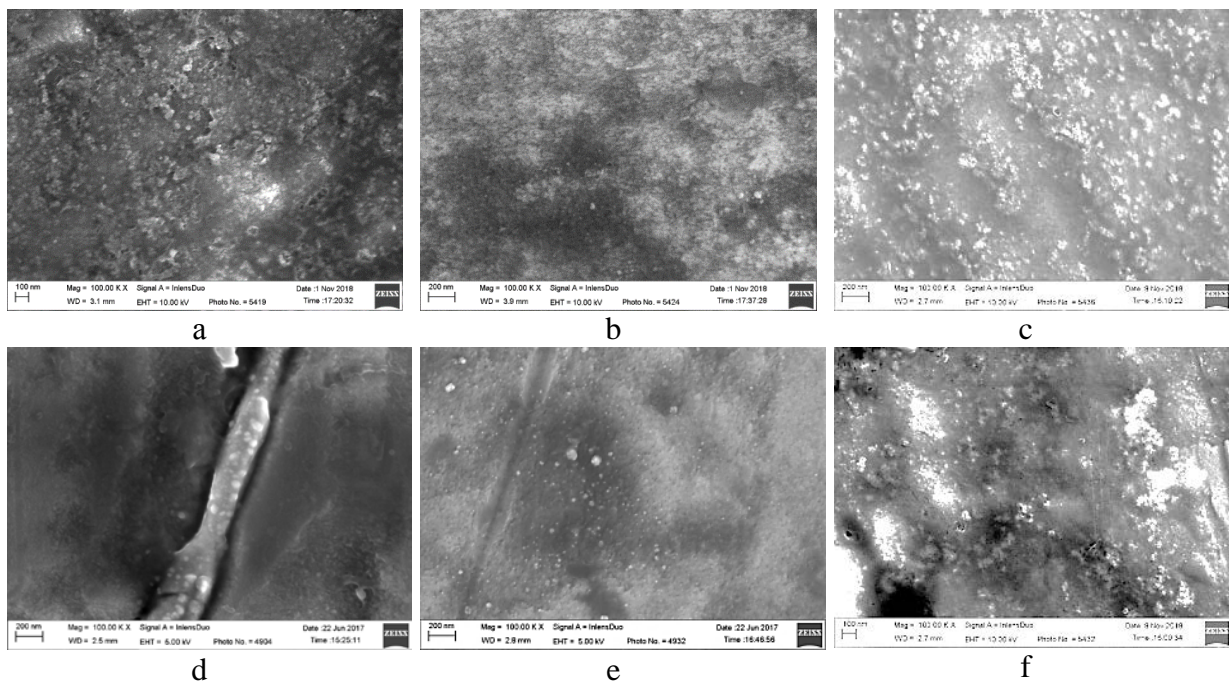


Fig. 7. SEM image of the cross section of the alloy (a, b, c) and welded joint (d, e, f) without thermal processing (a, d), and with it: quenching (b, e), artificial ageing (c, f).
Magnification $100\,000^{\times}$

After the artificial ageing at 170°C within 32 hours, the light particles with the characteristics size of 10 – 20 nm and 50 – 100 nm form in the matrix of the solid solution of both alloy and welded joint (Fig. 6 and 7, c, f).

The aluminum alloy B-1461 of the system Al-Cu-Li consists of the α -solid solution with the following phases inserted in the solid solution matrix: δ' (Al₃Li), T₁(Al₂CuLi), θ'' , θ' (Al₂Cu), Al₃(Zr Sc), and the phase over the boundaries of the dendritic grains T₁(Al₂CuLi), T₂(Al₆CuLi₃), S₁(Al₂MgLi), θ (Al₂Cu) [17]. The major strengthening phases are δ' (Al₃Li), T₁(Al₂CuLi), and θ' (Al₂Cu).

The laser welding results in the changes in the welded joint structure and dramatic reduction of its strength. Using these and other authors' results we can suggest that during the laser welding, the alloying elements like Cu, Mg, Li emit on the boundaries of the dendritic grains and form different phases. It is known that the electronic microscope shows in the back-scattered mode the light elements with the dark color, and heavy elements with the light color. We can also suggest that there is S₁(Al₂MgLi) in the dark agglomerates, and copper-containing phases T₁(Al₂CuLi), T₂(Al₆CuLi₃), θ (Al₂Cu) in the light agglomerates. The

quenching of the welded joint changes its microstructure, the contrast of the dendritic structure disappears, and the alloying elements diffusion results in the formation of the oversaturated solid solution, while σ_{UTS} rises in the welded samples. However the yield stress value σ_{YS} remains low. The artificial ageing results in the disintegration of the oversaturated solid solution and formation of strengthening phases in the matrix. Basing on the results of the microstructure analysis, we can suggest that at the optimal artificial ageing (170°C, 32 hours) the copper-containing phases T_1 and θ with the characteristic sizes of 10 – 20 nm emit and distribute uniformly in the solid solution matrix (see Fig. 7, c, f). The strength reaches its maximum after this processing – 510 MPa, plus extra 10% as compared to the quenching. At the same time, $\sigma_{0.2}$ rises even more – up to 430 MPa, i.e. by 1.32 times as compared to the quenching, as the elasticity halves.

Conclusions

The paper presents the investigations of the effect of the thermal processing on the mechanical characteristics (elasticity and tensile strength) and the microstructure of the welded connections for the aluminum alloy V-1461 of the system Al-Cu-Li. The thermal post-processing (quenching and artificial ageing) temperature and time characteristics were optimized in order to have the values of the tensile stress, yield stress and ultimate relative elongation, as well as to obtain the microstructure approaching to the respective characteristics of the basic alloy.

The regularities in the varying mechanical characteristics and microstructure of the welded joint were found for the laser-welded samples (the alloy V-1461 of the system Al-Cu-Li) regarding the thermal processing (quenching and artificial ageing). The regularities in the curve behavior show the clear maximums and minimums versus the temperature and time characteristics of the artificial ageing process. At the optimal modes of the thermal processing, the strengthening phases T_1 (Al_2CuLi), θ (Al_2Cu), T_2 (Al_6CuLi_3) form in the solid solution, whereas the tensile stress, yield stress and relative elongation of the welded sample are 0.92; 0.91 and 0.88 respectively against the basic alloy. Hence, controlling the parameters of the thermal processing of the samples, one can persistently influence the forming preset mechanical properties of the welded samples by means of the variation of the structural and phase composition of the welded joint.

Acknowledgements. *The work is supported by the grant of the Russian Scientific Foundation No. 17-79-20139. The study was conducted at the Joint Access Center «Mechanics» of ITAM SB RAS.*

References

- [1] Rioja RJ, Liu J. The evolution of Al-Li base products for aerospace and space applications. *Metallurgical and Materials Transactions A*. 2012;43(9): 3325-3337.
- [2] Dursun T, Soutis C. Recent developments in advanced aircraft aluminium alloys. *Materials & Design*. 2014;56: 862-871.
- [3] Abd El-Aty A, Xu Y, Guo X, Zhang SH, Ma Y, Chen D. Strengthening mechanisms, deformation behavior, and anisotropic mechanical properties of Al-Li alloys: A review. *Journal of Advanced Research*. 2018;10: 49-67.
- [4] Kashaev N, Ventzke V, Çam G. Prospects of laser beam welding and friction stir welding processes for aluminum airframe structural applications. *Journal of Manufacturing Processes*. 2018;36: 571-600.
- [5] Xiao R, Zhang X. Problems and issues in laser beam welding of aluminum-lithium alloys. *Journal of Manufacturing Processes*. 2014;16(2): 166-175.
- [6] Hu YN, Wu SC, Chen L. Review on failure behaviors of fusion welded high-strength Al

- alloys due to fine equiaxed zone. *Engineering Fracture Mechanics*. 2019;208: 45-71.
- [7] Cui L, Li X, He D, Chen L, Gong S. Effect of Nd:YAG laser welding on microstructure and hardness of an Al–Li based alloy. *Materials Characterization*. 2012;71: 95-102.
- [8] Gu C, Wei Y, Zhan X et al. Investigation of welding parameters on microstructure and mechanical properties of laser beam-welded joint of 2060 Al–Cu–Li alloy. *The International Journal of Advanced Manufacturing Technology*. 2017;91(1-4): 771-780.
- [9] Zhang X, Yang W, Xiao R. Microstructure and mechanical properties of laser beam welded Al-Li alloy 2060 with Al-Mg filler wire. *Materials & Design*. 2015;88: 446-450.
- [10] Fu B, Qin G, Meng X, Ji Y, Zou Y, Lei Z. Microstructure and mechanical properties of newly developed aluminum-lithium alloy 2A97 welded by fiber laser. *Materials Science and Engineering: A*. 2014;617(1): 1-11.
- [11] Zhang X, Huang T, Yang W, Xiao R, Liu Z, Li L. Microstructure and mechanical properties of laser beam-welded AA2060 Al-Li alloy. *Journal of Materials Processing Technology*. 2016;237: 301-308.
- [12] Orishich AM, Malikov AG, Karpov EV, Pavlov NA, Mesenzova IS. Effect of Heat Treatment on Mechanical and Microstructural Properties of the Welded Joint of the Al–Mg–Li Alloy Obtained by Laser Welding. *Journal of Applied Mechanics and Technical Physics*. 2018;59(3): 561-568.
- [13] Annin BD, Fomin VM, Karpov E V., Malikov AG, Orishich AM. Effect of Mg and Cu on mechanical properties of high-strength welded joints of aluminum alloys obtained by laser welding. *Journal of Applied Mechanics and Technical Physics*. 2017;58(5): 939-946.
- [14] Orishich A, Malikov A, Karpov E. Analysis of the effect of the thermomechanical processing on the laser weld joint of aluminum alloys of Al-Mg-Li and Al-Cu-Li. *Procedia CIRP*. 2018;74: 442-445.
- [15] Malikov A, Orishich A, Karpov E, Sandalov E. Increase of the Elasticity and Strength of the Welded Joints for the Al-Mg-Li Alloy Made by the Laser Welding by Means of the Thermal Mechanical Processing. *Defect and Diffusion Forum*. 2018;385: 385-390.
- [16] Kaigorodova LI, Rasposienko DY, Pushin VG, Pilyugin VP, Smirnov SV. Influence of Severe Plastic Deformation on the Structure and Properties of Al–Li–Cu–Mg–Zr–Sc–Zn Alloy. *Physics of Metals and Metallography*. 2018;119(2): 161-168.
- [17] Khokhlatova LB, Kolobnev NI, Oglodkov MS, Lukina EA, Sbitneva SV. Change in phase composition in relation to aging regimes and alloy V-1461 semifinished product structure. *Metal Science and Heat Treatment*. 2012;54(5-6): 285-289.
- [18] Khokhlatova LB, Kolobnev NI, Oglodkov MS, Mikhaylov ED. Aluminum-lithium alloys for aircraft building. *Metallurgist*. 2012;56(5-6): 336-341.
- [19] Oliveira PI, Costa JM, Loureiro A. Effect of laser beam welding parameters on morphology and strength of dissimilar AA2024/AA7075 T-joints. *Journal of Manufacturing Processes*. 2018;35: 149-160.
- [20] Zhang X, Liu B, Zhou X et al. Laser welding introduced segregation and its influence on the corrosion behaviour of Al-Cu-Li alloy. *Corrosion Science*. 2018;135: 177-191.